JOURNAL OF MATERIALS SCIENCE 20 (1985) 3289 – 3299

Some advantages of carbon paste electrodes in the morphological study of finely divided iron oxides

M. T. MOUHANDESS, F. CHASSAGNEUX, B. DURAND*
Laboratoire de Chimie Minérale III, Université Claude Bernard Lyon I, 43 Bd du 11 Novembre 1918, 69622 Villeurbanne Cedex, France

Z. Z. SHARARA, O. VITTORI
Laboratoire de Chimie Analytique III, Université Claude Bernard Lyon I, 43 Bd du 11 Novembre 1918, 69622 Villeurbanne Cedex, France

The electroreduction of finely divided trivalent iron oxides using a carbon paste electrode occurs according to a mechanism involving the dissolution of the solid and then the reduction of solvated Fe^{3+} ions into Fe^{2+} ions. The voltammetric curves exhibit two peaks. The first is due to the reduction of Fe^{3+} ions that come from dissolution of the smallest particles at the beginning of the experiment. The second is characteristic of reduction of the solid; its shape, position and amplitude are influenced by morphology. Theoretical aspects are considered. It appears that the use of a carbon paste electrode for the study of divided solids containing an electroreactive ion can easily give information either on the particle size distribution, if the dissolution kinetics of the compound are known, or on the dissolution kinetics of monodisperse solids or solids whose particle size distribution is well defined.

1. Introduction

Difficulties in morphological studies arise from the number of experiments required, the variety of methods available for application and also the interpretation of the data, especially when solids with a wide granulometric range are concerned.

X-ray analysis leads to some information on the mean size of crystallites by measuring the broadening of the diffraction peaks, but it is rather difficult to be completely satisfied for sizes above 0.1 μm. Information on particle shapes, on shape and size homogeneity, on inter-crystallite or intra-crystallite porosity and on microcrystalline phases possibly present is available from electron microscopy. Other techniques such as BET or mercury porosimetry give more detail on surface state and particle size.

The size distribution may be obtained with devices using Stokes's law and measuring the diameters of powder particles when in suspension in a suitable liquid. Some devices use vertical sedimentation and it is then possible to study particles having a diameter between about 10 and 100 μm. The measuring time is rather long for finely divided powders. Other apparatus uses horizontal sedimentation accelerated by centrifugation. This leads to shorter measuring times and allows size evaluation as low as 0.01 μm. The usual measuring range is between 0.01 and 100 μm. Powders are mixed with an appropriate solvent and suspension is achieved using an

*To whom correspondence should be addressed.

0022–2461/85 $03.00 + .12

ultrasonic device. The measurements are then performed, as for electron microscopy, on very small samples. The major difficulty arises from the reproducibility and the representativeness of the sampling.

All these techniques require expensive apparatus and are not always available in laboratories. In the present paper, we shall describe the applicability of a carbon paste electrode to morphological studies of several divided powders, outlining the low cost of electrochemical equipment and the ease with which the device is used.

2. Historical aspects

First described by Adams in 1958 [1, 2] the carbon paste electrode has been widely used in electrochemical investigations. Several technological characteristics have been proposed in order to obtain valuable data. The electrode is a mixture of carbon powder with the solid under study, and is prepared with a liquid binder that is either conducting or not [3–5]. In the first case, the electrical charge flowing through the electrode may be very important because the whole incorporated solid may be transformed into reduced (or oxidized) species [4, 5]. From examination of the voltammetric curves, either in the cathodic or the anodic direction, numerous works have described the study of inorganic solids: characterization of phases, determination of elements or of oxidation state, and stoichiometry [3, 5–7]. So it appears that electrochemical behaviour is closely related to the nature of the electroactive solid. However, it is well known that solid reactivity is related not only to structure and stoichiometry but also to morphology [8]. Bauer *et al.* [5] have described the electrochemical reduction of copper sulphides and pointed out that it may become partial when the particle size increases. More recently, Lenglet [9] has outlined the great influence of sample synthesis, as well as subsequent thermal treatment, on the interpretation of voltammetric data. But the influence of morphology has only been fully taken into account more recently by Mouhandess *et al.* [10–13] and Sharara *et al.* [14–17], who have studied the electrochemical behaviour of simple or mixed iron(III) oxides, when introduced into a carbon paste electrode with conducting binder. By systematic work on the synthesis parameters, they have shown very interesting variations of electrochemical behaviour.

3. Technology

3.1. Electrode preparation

The working electrode (Fig. 1) is made up of a vitreous carbon rod sealed in a polytetrafluoroethylene (PTFE) pipe so as to leave a small cavity at the bottom (1 mm depth and the same diameter as the vitreous carbon rod, 3 mm). This cavity is filled with the carbon paste, which is pressed in slightly with a spatula. The paste is prepared from a "high-purity graphite" (ash less than 2 p.p.m.) available from Le Carbone Lorraine (ref. 9901). A granulometric examination of this powder shows that 85% of the particles have a diameter in the 12 to 28 μm range; about 11% are smaller and 4% larger. The paste is made up of 95 mg of graphite powder, 5 mg of the oxide under study and 50 μl of binder, usually a 1 M HCl aqueous solution. Such a composition allows complete reduction of haematite [10]. An average of 15 mg of this paste is placed in the electrode cavity.

This kind of electrode, according to Lindquist [18], exhibits several advantages over solid ones: small residual current, large electroactivity range and easy replacement of the paste.

3.2. Cell and apparatus

The cell is provided with a water jacket in order to keep the temperature fixed. The now-classical three-electrode configuration is used here with the carbon paste electrode as working electrode, a saturated calomel electrode (SCE) as reference and a platinum wire as auxiliary. Bubbling of

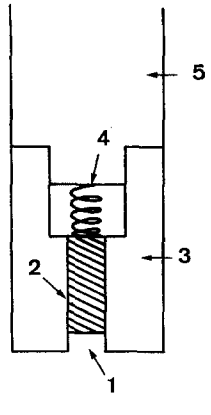

Figure 1 Carbon paste electrode tip: 1, cylindrical cavity (3 mm diameter and 1 mm depth); 2, glassy carbon rod; 3, Teflon body; 4, electrical contact; 5, metallic rod.

nitrogen removes oxygen from the bulk and a nitrogen pressure is always applied during the course of an experiment in order to avoid any parasitic reduction of soluble oxygen.

A PRG5 pulse polarograph is used as potential function generator, coupled with an ELP2 recorder, a TV11GD plug-in and a PHN81 millivoltmeter, all available from Solea-Tacussel (72 rue d'Alsace, 69700 Villeurbanne, France).

Supporting electrolyte and binder are identical and are strong inorganic acid solutions, usually 1 M, which are not electrochemically reduced or oxidized in the electroactive range, between -0.8 and $+1.1$ V/SCE. Hydrochloric acid is used most frequently.

3.3. Synthesis of iron oxides

Haematite samples (αFe_2O_3) were prepared by firing in air, at temperatures between 500 and 900° C, three iron(III) compounds: the sesquioxide (Merck, ref. 3924), ferric oxide precipitated by ammonia and ammonium trioxalatoferrate.

Samples of magnetite were prepared either by pyrolysis of ammonium trioxalatoferrate in a controlled reducing atmosphere or by the reaction of a fused iron(II) salt with sodium ferrite, $NaFeO_2$.

Alkaline ferrites, $LiFeO_2$ and $NaFeO_2$, were synthesized by thermal treatment in solid phase of mixtures of finely divided haematite and the respective alkali carbonate.

Samples of cobalt and zinc ferrites ($CoFe_2O_4$ and $ZnFe_2O_4$) were obtained by double decomposition reactions between a cobalt or zinc fused salt and an alkaline ferrite at temperatures between 400 and 900° C.

These oxides have very different morphologies, but all are made up of very small crystallites, the size of which was between several tens to several hundreds nanometres.

4. General aspect of voltammetric curves

The voltammetric curves recorded for the samples described above usually exhibited some similarity. As an example, the behaviour in 1 M HCl of a haematite sample ground for 8 h is shown in Fig. 2. There are two effects to be discussed:

(a) The first one, corresponding to peaks P_1, P_3, P_4, ..., is due to a reversible charge transfer

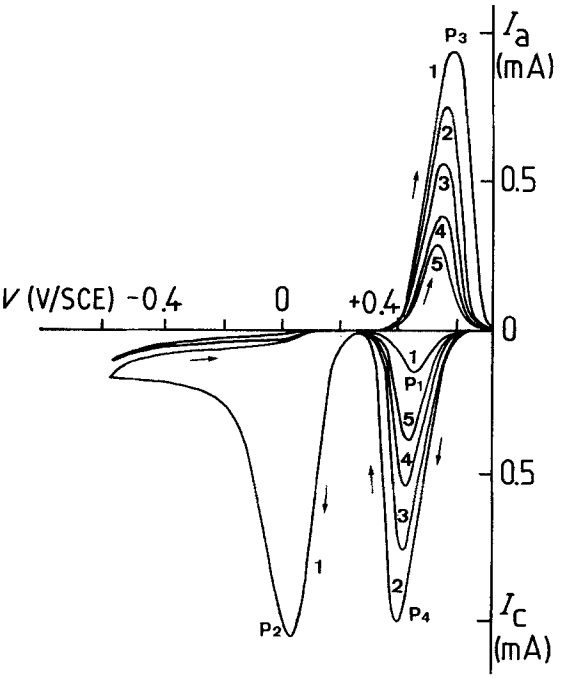

Figure 2 Cyclic voltammetric curves with iron oxide, αFe_2O_3, incorporated in carbon paste, obtained from $(NH_4)_3[Fe(C_2O_4)_3] \cdot 3H_2O$ at 500° C and ground for 8 h. Supporting electrolyte and binder is 1 M HCl. Numbers on the curves indicate the successive potential sweeps ($120\,mV\,min^{-1}$).

close to the normal potential of the Fe^{3+}/Fe^{2+} couple in hydrochloric medium. In fact, these peaks are noticed for all samples, even if the supporting electrolyte is changed, leading only to a slight shift of the potential values. One may then conclude that these peaks are related to the iron ions from the instantaneous chemical dissolution of the finest particles when preparing the carbon paste electrode.

(b) The second one, corresponding to peak P_2, is due to an irreversible step attributed to the electrochemical reduction of the solid oxide. The peak potential and the shape of the peak are quite different from one sample to another, and so may be characteristic of a given sample.

Iron(II) ions present in the solution after a cathodic sweep, up to potentials more negative than that of peak P_2, have been determined by pulse polarography (the paste is then dispersed in the bulk to give homogeneous solution) [19]. The electrical charges measured in this way are in good agreement with that measured from the area of peaks P_1 and P_2. This explains why peak P_3 is larger than P_1; the Fe^{2+} ions produced

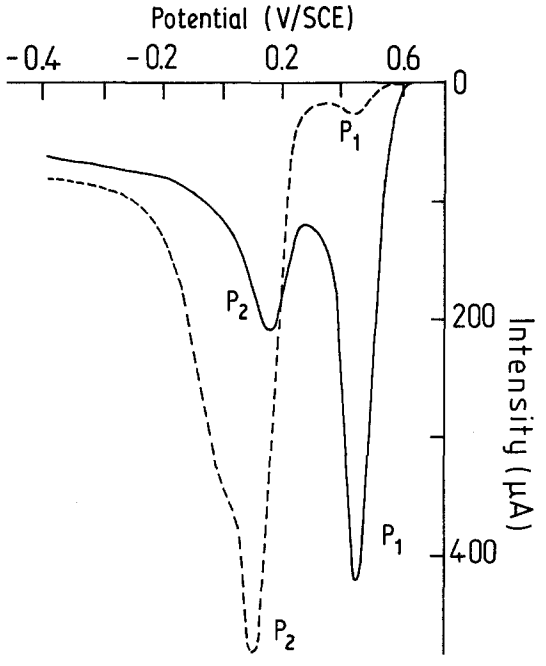

Figure 3 Voltammetric curves of alkaline ferrites in 1 M HCl: full curve, $NaFeO_2$; broken curve, $LiFeO_2$. Potential sweep rate is 12 mV min^{-1}.

during the cathodic sweep (P_1, P_2) stay in the paste and are oxidized (P_3) when the sweep is made anodic. In fact, some of the Fe^{2+} ions diffuse towards the bulk and this is well illustrated by successive cyclic sweeps between +0.2 and +0.7 V/SCE.

Modifications of the voltammetric curves when experimental parameters are changed, such as pH and nature of the supporting electrolyte and binder, have led first Mouhandess *et al.* [10] and then Sharara *et al.* [14, 17] to confirm that the electrochemical dissolution of simple or mixed iron oxides is a chemical–electrochemical mechanism. The first step is the chemical dissolution of the solid, with low kinetics. The second, electrochemical step, is the fast reduction of iron(III) ions into iron(II). Such a mechanism has previously been suggested by both Lamache and Bauer [20] and Laviron [21, 22] for ferrocene oxidation or vanadium oxide reduction.

One may thus observe that the electrochemical behaviour of finely divided oxides is essentially related to the kinetics of dissolution. In Fig. 3 are shown the voltammetric curves for two samples of lithium and sodium ferrites, $LiFeO_2$ and $NaFeO_2$, obtained in the same way. For $NaFeO_2$, well known to be more easily hydrolysable than $LiFeO_2$ [23, 24], one can see that peak P_1 is larger than peak P_2 and that the difference between peak potentials, $E(P_2) - E(P_1)$, is small. In contrast, $LiFeO_2$ exhibits a quite different behaviour, with peak P_2 larger than peak P_1 and situated at a lower potential. One may thus conclude that, for slightly soluble compounds, solid morphology will have a large influence on peak P_2.

5. Evidence for influence of morphology

Now we are only concerned with peak P_2 due to the electrochemical reduction of the oxide, according to the chemical–electrochemical mechanism described above. All the voltammetric curves are recorded from +0.3 to −0.7 V/SCE in one cathodic sweep, with 15 mV min^{-1} for the sweep rate and 1 M HCl as supporting electrolyte as well as binder.

Four haematite samples have been studied, characterized by obvious morphological differences (Table I, Fig. 4). The voltammetric curves exhibit various shapes as shown in Fig. 5: one peak, two peaks, or a wave. (Despite the fact that reduction currents are usually taken as negative, in the following discussion we assume that the maximum of a peak is the point where

TABLE I Parameters of four αFe_2O_3 samples

Sample	Sample obtained from	Particles less than 10 μm (%)	Crystallite size (nm)	Electrochemical reduction efficiencies (%)
A	αFeOOH "Bayer" 315° C ground	100	25	100
B	Trioxalic complex 500° C	100	60	100
C	αFeOOH 500° C	85	20	40
D	Trioxalic complex 1015° C	75	⩾ 100	15

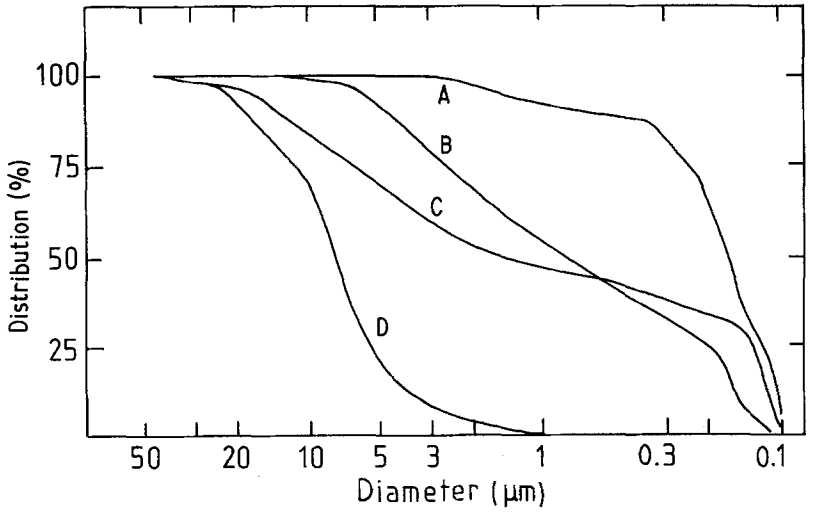

Figure 4 Granulometric distribution obtained with Sedigraph 5000 for four samples of αFe_2O_3 synthesized as follows: Sample A, by dehydration of FeOOH "Bayer" at 315° C and ground; Sample B, by pyrolysis of oxalic complex at 500° C; Sample C, by dehydration of FeOOH, laboratory synthesized, at 500° C; and Sample D, by pyrolysis of oxalic complex at 1015° C.

the absolute value of the intensity is maximum.) Several remarks arise from the examination of Figs. 4 and 5.

1. The reduction peak is larger and sharper when the granulometric distribution is narrow and centred on a very small value of the mean diameter (Figs. 4, Curve A, and 5, Curve A). In contrast, when the granulometric distribution is broad with a mean diameter larger than 1 μm, the peaks are broad and less intense (Figs. 4, Curve B, and 5, Curve B). We notice that the electrochemical reduction efficiency is 100% for the samples with the finest particles.

2. The reduction appears to be a wave shifted towards negative potential values for the sample annealed at 1000° C which contains a lot of particles with mean diameter larger than 10 μm (Figs. 4, Curve D, and 5, Curve D). The reduction is only partial in this case.

3. For sample C, characterized by a granulometric distribution with two mean diameters, the voltammetric curve exhibits two peaks (Figs. 4, Curve C, and 5, Curve C) and the electrochemical efficiency is less than 100%.

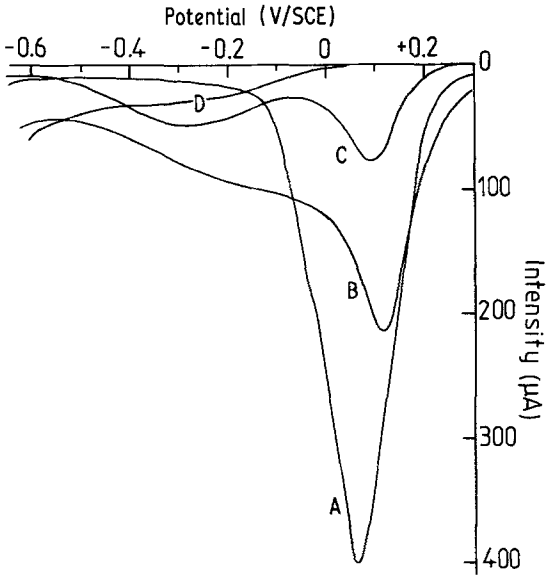

Figure 5 Voltammetric curves of samples of Fig. 4. Binder and supporting electrolyte is 1 M HCl; $v = 15\,mV\,min^{-1}$.

For a haematite sample, αFe_2O_3 with a corundum structure, synthesis influences both shape and peak potential, as well as electrochemical efficiency [11–13]. In addition, for a given sample, any thermal treatment or grinding modifies the voltammetric curve. The more the solid is finely divided, the more the electrochemical yield increases and the more the peak is shifted towards positive potential. Usually the reduction peak is in the +0.15 to −0.4 V/SCE range.

The behaviour of cobalt ferrite, $CoFe_2O_4$ [15], is identical to that of haematite, as shown in Fig. 6 and Table II, for cobalt ferrite samples obtained from the reaction of sodium ferrite

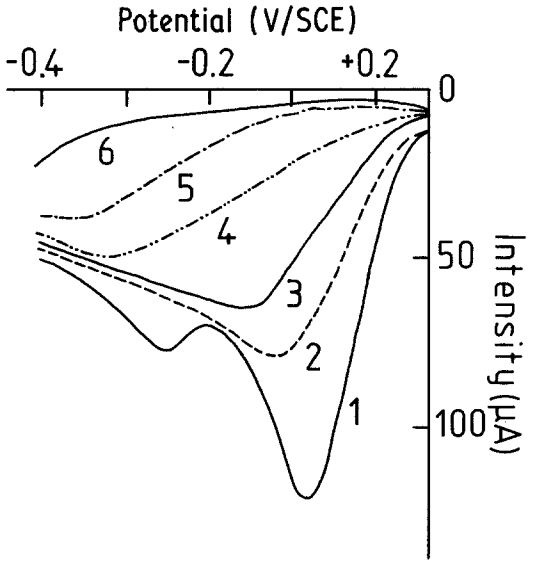

Figure 6 Voltammetric curves of cobalt ferrite prepared from sodium ferrite at different temperatures (v = 12 mV min^{-1}, 1 M HCl). The sample numbers are the same as in Table II.

with a cobalt salt at various temperatures. In the present case, an increase of the synthesis temperature leads to a progressive decrease of the peak magnitude, and consequently of the electrochemical efficiency. In addition the peak potential is slightly shifted towards more negative values, and the peak becomes a wave. An increase of the mean diameter of the crystallites and of the size of the particles is observed and confirmed by other techniques (X-ray and electron microscopy). We note here that a difference between crystallite and particle exists, a particle being made up of several crystallites. A double peak shape is observed for the sample prepared at 400° C and it is obvious that a granulometric partition, with two kinds of sizes having two very different mean diameters, is the cause of this observation (Figs. 6, Curve 1 and 7a). One of these diameters is smaller than that of the sample prepared at 600° C (Fig. 7b) and the second is larger.

The behaviour of zinc ferrite, $ZnFe_2O_4$ [16], is different to that of cobalt ferrite (Fig. 8, Table II). The increase of temperature from 400 to 600° C is shown to be very advantageous for the electrochemical efficiency, since the magnitude of the peak increases and the maximum potential is shifted towards more positive values, despite an increase of the mean crystallite diameter. But above 600° C the phenomenon is reversed, as for $CoFe_2O_4$.

A careful study of the electron micrographs shows clearly that this difference of behaviour is easily explainable: a great contrast exists between cobalt ferrite (Figs. 7a and b) and zinc ferrite (Figs. 7c and d). Cobalt ferrite is made up of fine particles relatively well individualized whereas zinc ferrite is made up of irregular and larger particles, with superficial cracks. The size of these aggregates decreases as the temperature

TABLE II Temperature dependence of electrochemical reactivity for cobalt and zinc ferrites

(a) Cobalt: $2NaFeO_2 + Co^{2+} \xrightarrow{\theta, t} CoFe_2O_4 + 2Na^+$

Synthesis temperature (° C)	Time (h)	E peak (V/SCE)	Reduction efficiency (%)	Crystallite diameter (nm)	Sample number*
400	96	+0.04	68	19	1
500	48	−0.03	47	20	2
600	48	−0.10	34	74	3
700	24	−0.44	20	94	4
800	24	−0.50	8	–	5
900	24	–	–	–	6

(b) Zinc: $2NaFeO_2 + Zn^{2+} \xrightarrow{\theta, t} ZnFe_2O_4 + 2Na^+$

Synthesis temperature (° C)	Time (h)	E peak (V/SCE)	Reduction efficiency (%)	Crystallite diameter (nm)	Sample number*
400	40	−0.06	59	22	7
500	40	−0.05	68	32	8
600	40	−0.04	78	62	9
800	40	−0.06	29	90	10

*Sample numbers are reported in Figs. 6, 7 and 8.

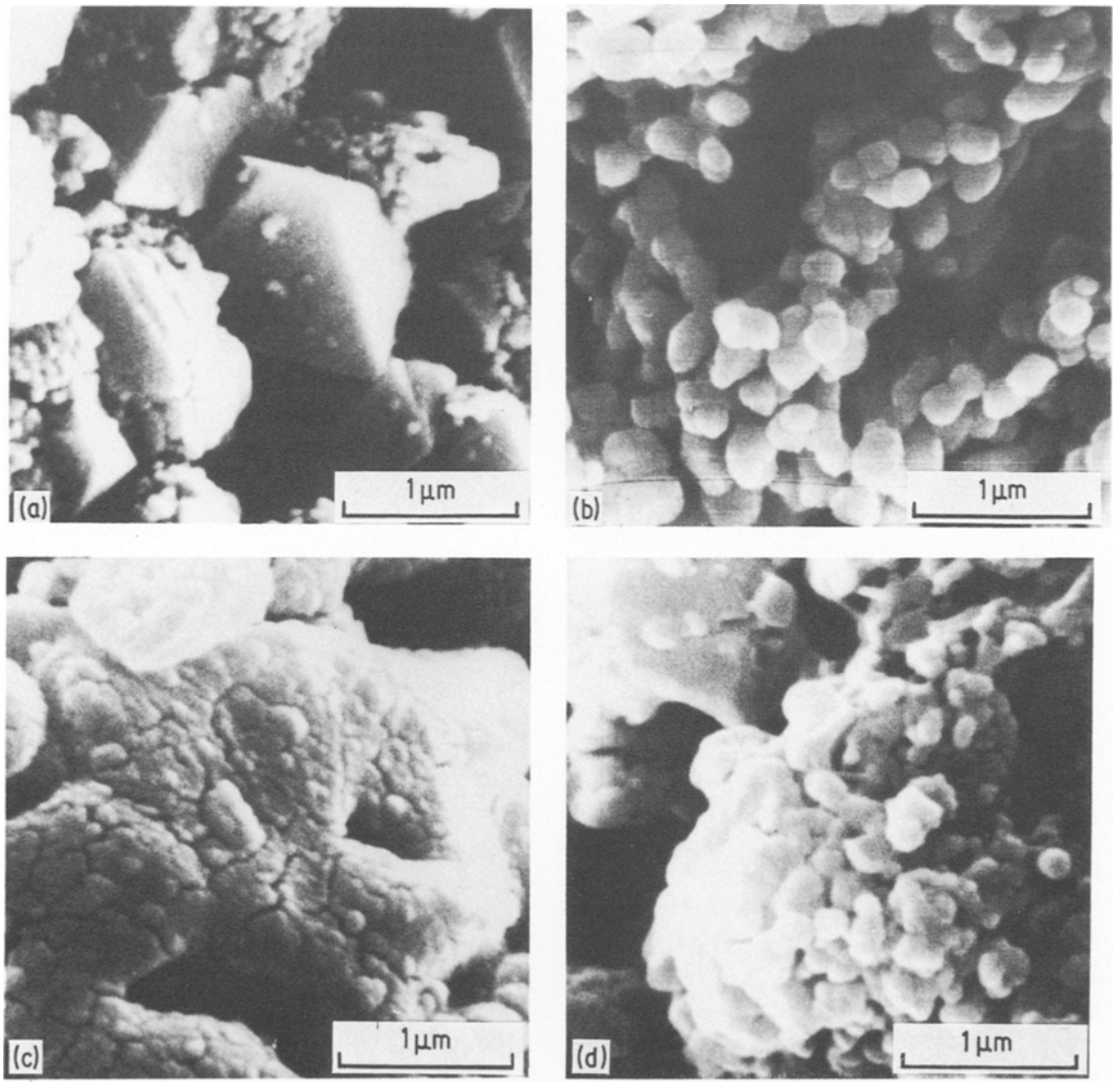

Figure 7 Electron micrograph of the ferrite samples described in Table II: (a) Sample 1; (b) Sample 3; (c) Sample 7; (d) Sample 9.

is increased from 400 to 600° C, and the electrochemical efficiency simultaneously increases, outlining clearly that electrochemical behaviour is influenced more by habitat than by elementary crystallite size. Moreover, one can easily understand that long mechanical grinding breaks these aggregates into smaller particles, the size of which varies in the same way as that of crystallites, and so that it is the inverse of the evolution of electrical yields as actually observed. We see also, in Fig. 9, the effect of thermal treatment on these aggregates; annealing at 600° C for 20 h of a sample prepared at 500° C leads to agglomeration which involves the disappearance of the reduction peak. But it is not truly a sintering because electrochemical reduction takes place again after a short grinding.

So the contrasting behaviour of these oxides of spinel structure is related to their morphology. In both cases the reduction is enhanced and shifted in the anodic sense as the particle sizes became smaller. The cathodic dissolution is in the $+0.2$ to -0.5 V/SCE range. The solubility of cobalt and zinc ferrite in 1 M HCl seems to be of the same magnitude as for haematite.

Magnetite and maghaemite, both of cubic spinel structure, as well as alkaline ferrites, $LiFeO_2$ and $NaFeO_2$, have a different behaviour

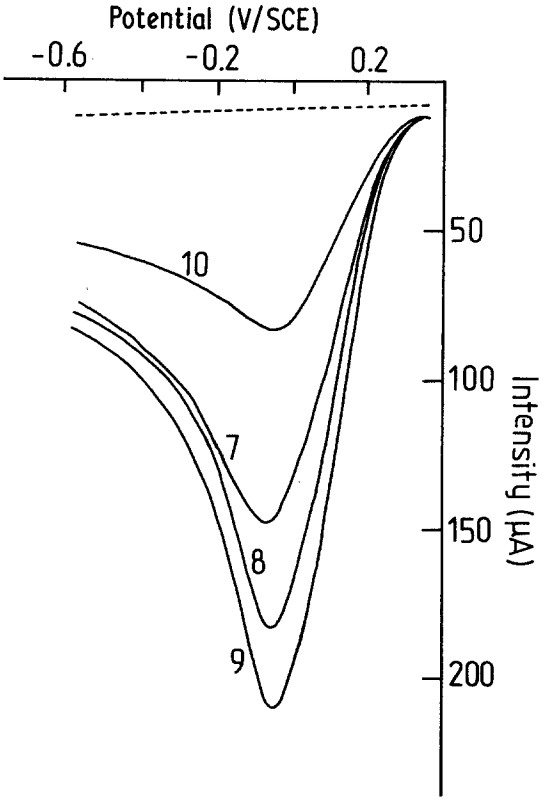

Figure 8 Voltammetric curves of zinc ferrite prepared from sodium ferrite at different temperatures (12 mV min^{-1}, 1 M HCl). The sample numbers are the same as in Table II.

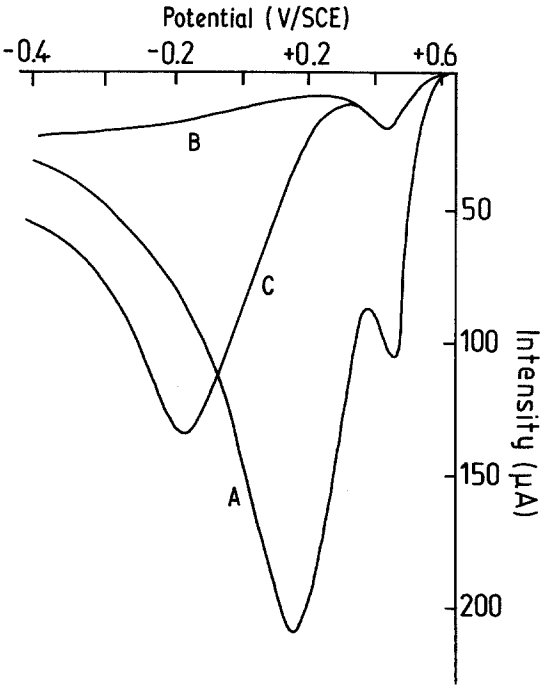

Figure 9 Influence of annealing treatment at 600° C in solid phase and then of grinding on a zinc ferrite sample prepared at 500° C: Curve A, initial sample; Curve B, after annealing at 600° C; Curve C, after grinding.

from the above oxides. The reduction is always complete. The cathodic peak is either sharp or broad and sometimes a second peak or a shoulder is noticed but not a wave. So we conclude that these four oxides dissolve more quickly in 1 M HCl medium than αFe_2O_3, $CoFe_2O_4$ and $ZnFe_2O_2$.

In addition, for magnetite, maghaemite, $LiFeO_2$ and $NaFeO_2$, the reduction potential range is closer to that of the Fe^{3+}/Fe^{2+} couple (Fe_3O_4, +0.3 to +0.2 V/SCE; γFe_2O_3, +0.2 to +0.16 V/SCE; $LiFeO_2$, +0.2 to +0.07 V/SCE; and $NaFeO_2$, +0.18 to +0.15 V/SCE). The shoulder sometimes observed on the peak seems to be due to a granulometric distribution of the sample, divided into two populations of particles, as shown on the histogram obtained with the Horiba Capa 500 particle size analyser (Fig. 10).

6. Equation of electroreduction curves

Since electroreduction is related to the kinetics of dissolution of the solid (either simple or mixed iron(III) oxides) and then to the reduction of iron(III) into iron(II), an equation may be proposed to explain the electrochemical behaviour of haematite, αFe_2O_3. According to Delmon [25], the dissolution rate may be expressed as:

$$\frac{dx}{dt} = 3\frac{K_i}{r_0}\frac{S}{S_0} \quad (1)$$

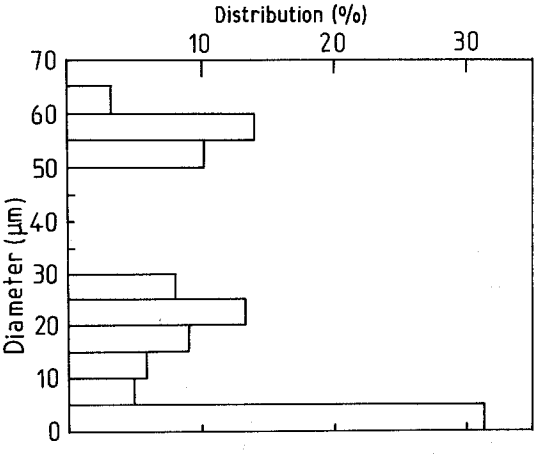

Figure 10 Size distribution of a sample of $LiFeO_2$.

In Equation 1, x is the dissolved fraction of iron oxide at time t. This oxide is assumed to be made up of N spherical particles of only one size characterized by radius r_0. S_0 and S are the surface at time zero and t. K_i is the specific interfacial rate and may be written [26, 27]:

$$K_i = K_0[Fe^{2+}]^a[Fe^{3+}]^{-a} \quad (2)$$

with $a \simeq 0.5$. Constant K_0 depends on H^+ and Cl^- concentrations. Calculations published elsewhere [10, 28] lead to a general equation for the current potential curve at any time after the potential sweep has been applied:

$$i = A\left[\exp\left(\frac{anFvt}{RT}\right)\right] \times\left\{\frac{ART}{3anFv}\left[1 - \exp\left(\frac{anFvt}{RT}\right)\right] + Q_0^{1/3}\right\}^2 \quad (3)$$

In Equation 3, v is the potential sweep rate, Q_0 the equivalent charge of the oxide, and A a constant related to K_0, r_0, $E^\circ_{Fe^{3+}/Fe^{2+}}$ and the initial starting potential E_i, as follows:

$$A = 3K_0\left(\frac{Q_0^{1/3}}{r_0}\right)\exp\left(\frac{anF}{RT}\right)(E^\circ - E_i) \quad (4)$$

Equations 3 and 4 only apply to an ideal monodisperse oxide powder. But usually synthesis procedures lead to samples having a wide range of sizes. So it is obvious that one may consider such a powder as the mixture of several classes, characterized by one radius and a given percentage p_j of the total amount of charge Q_0 ($Q_j = p_jQ_0$). The current flowing through the electrode may be written as:

$$i_T = \sum_{j=1}^{j=n} A_j\left[\exp\left(\frac{anFvt}{RT}\right)\right]\left\{\frac{AjRT}{3anFv} \times\left[1 - \exp\left(\frac{anFvt}{RT}\right)\right] + Q_j^{1/3}\right\}^2 \quad (5)$$

In Equation 5, n is the chosen number of classes, A_j being Equation 4 adjusted for Q_j and r_j. Simulation curves have been computed for Samples A and C (Table I), using 20 classes for the granulometric distribution (Fig. 4), and have been compared with experimental curves

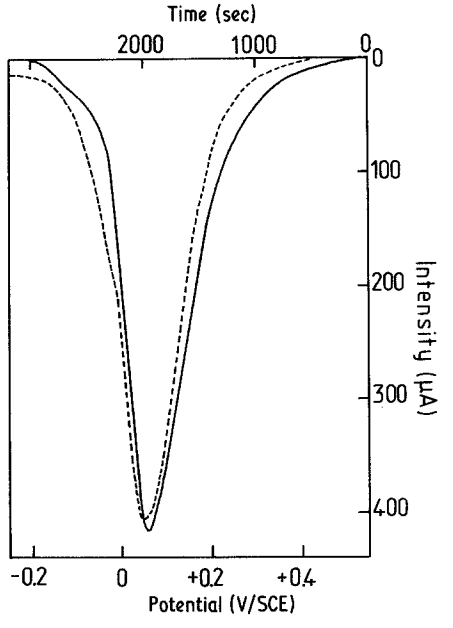

Figure 11 Comparison of experimental (----) and calculated (—) curves for αFe_2O_3 (same samples as Sample A in Fig. 4).

(Figs. 11 and 12). For Sample A, made of small particles (75 wt % less than 0.35 μm), the agreement is good. For Sample B, composed of particles whose distribution size is divided into two populations, the agreement between experimental and theoretical curves is less satisfactory

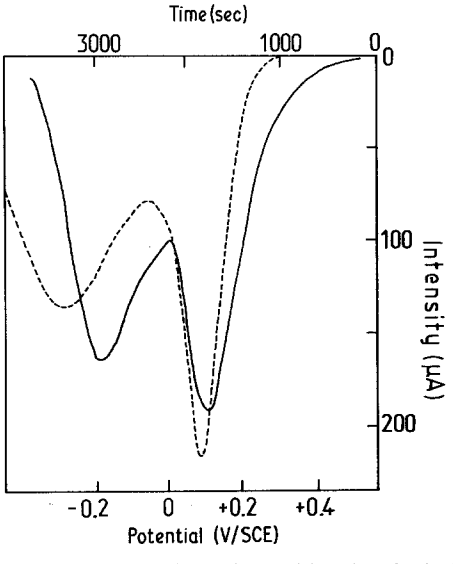

Figure 12 Comparison of experimental (----) and calculated (——) curves for αFeOOH (laboratory synthesized).

than above; but we notice that two peaks are observed, the first corresponding to the smallest particles, and having a better fitting curve than the second.

7. Conclusion

All the data reported here on the electrochemical behaviour of iron oxides, when incorporated in carbon paste electrodes with conducting binder, are interpreted as a chemical–electrochemical mechanism with chemical dissolution followed by electrochemical reduction of Fe^{3+} ions. This mechanism takes into account the effect of particle size and, despite some other morphological parameters, such as porosity and possible superficial perturbed layers, may be also dependent on the dissolution of oxides [29, 30]; the distribution size of particles certainly plays a leading part.

For haematite, under rather simple hypotheses, such as spherical particles with no porosity and homogeneous dissolution without any important diffusion effect, the voltammetric curves may be calculated and fitted to the experimental curves with acceptable accuracy. So it should be possible to obtain, to a good approximation, the granulometric distribution from the electrochemical behaviour of a divided sample incorporated in a carbon paste electrode. The agreement between experimental and calculated curves will certainly be improved, on the one hand, by a better knowledge of the granulometric distribution of the sample (minor empirical modifications are enough to reach an excellent curve fitting [28]) and, on the other hand, by an optimization of the above model taking into account other morphological parameters.

The theoretical aspect has been considered only for haematite because we are not sure that the other oxides comply with the same law; their electrochemical behaviour is indeed very similar, but we think that better knowledge of their dissolution kinetics is necessary.

Finally, for a monodisperse powder or for a powder whose granulometric characteristics are well known, the study of electrochemical behaviour is able to give information on the dissolution kinetics. Inversely, for solids whose dissolution kinetics are known, the carbon paste electrode leads easily to the granulometric distribution. We think also that the advantages of the carbon paste electrode, as illustrated in this paper, are not limited to iron(III) oxides; the technique might be applied to other divided solids, provided they may be reduced or oxidized in the electrochemical solvent range.

Acknowledgements

The authors wish to acknowledge helpful discussions with Professor J. Paris during the course of this work.

References

1. R. N. ADAMS, *Anal. Chem.* **30** (1958) 1576.
2. *Idem.*, "Electrochemistry at Solid Electrodes" (M. Dekker, New York, 1969).
3. J. M. LECUIRE, thesis, Nancy, 1974.
4. D. BAUER and PH. GAILLOCHET, *Electrochem. Acta* **19** (1974) 597.
5. M. C. BRAGE, M. LAMACHE and D. BAUER, *Analusis* **6** (7) (1978) 284.
6. P. GAILLOCHET, D. BAUER and M. C. HENION, *ibid.* **3** (9) (1975) 513.
7. J. M. LECUIRE and Y. PILLET, *J. Electroanal. Chem.* **91** (1978) 99.
8. A. ROUSSET, J. PARIS and F. CHASSAGNEUX, *Ann. Chim. Fr.* **4** (1979) 115.
9. P. FOULATIER and A. LENGLET, *Compt. Rend. Acad. Sci.* **289** (1979) 125.
10. M. T. MOUHANDESS, thesis, Lyon, 1983 (order number 83-82).
11. M. T. MOUHANDESS, F. CHASSAGNEUX and O. VITTORI, *Compt. Rend. Acad. Sci. Paris* **290** (1980) 267.
12. *Idem, J. Electroanal. Chem.* **131** (1982) 367.
13. *Idem, Compt. Rend. Acad. Sci. Paris* **294** (1980) 571.
14. Z. Z. SHARARA, thesis, Lyon, 1983 (order number 1374).
15. Z. Z. SHARARA, B. DURAND and O. VITTORI, *Compt. Rend. Acad. Sci. Paris* **298** (1984) 33.
16. *Idem, ibid.* **298** (1984) 445.
17. Z. Z. SHARARA, O. VITTORI and B. DURAND, *Electrochem. Acta* **29** (1984) 1685.
18. J. LINDQUIST, *J. Electroanal. Chem.* **52** (1974) 37.
19. O. VITTORI, *Techn. Ing.* **1** (1979) 2145.
20. M. LAMACHE and D. BAUER, *J. Electroanal. Chem.* **79** (1977) 359.
21. E. LAVIRON, *ibid.* **90** (1978) 33.
22. R. GAVASSO and E. LAVIRON, *ibid.* **102** (1979) 249.
23. R. COLLONGUES and J. THERY, *Bull. Soc. Chim. Fr.* **26** (1959) 1141.
24. J. THERY, *Ann. Chim. Fr.* **13** (1967) 7.
25. B. DELMON, "Introduction à la Cinétique Hétérogène, (édition Technip, Paris, 1969).
26. I. G. GORICHEV, N. A. KIPRIYANOV and V. F. GORSHENEVA, *Kin. Catal.* **20** (1979) 501.
27. I. G. GORICHEV, V. S. DUKHANIN and M. A. ZOLOTOV, *Sov. Electrochem.* **15** (9) (1980) 1118.

28. M. T. MOUHANDESS, F. CHASSAGNEUX, O. VITTORI, A. ACCARY and R. REEVES, *J. Electroanal. Chem.* **181** (1984) 93.
29. R. GOUT, F. SOUBIES, A. BOULEAU and C. LURDE, *Cah. ORSTOM, Sér. Pédol.* **12** (3/4) (1974) 289.
30. R. GOUT, F. SOUBIES, R. VICTOR, A. BOULEAU and C. LURDE, *ibid.* **18** (3) (1979) 225.

Received 24 July
and accepted 5 November 1984